Drug Delivery

DOI: 10.1002/ange.201409770

Noncanonical Amino Acids to Improve the pH Response of pHLIP Insertion at Tumor Acidity**

Joab O. Onyango, Michael S. Chung, Chee-Huat Eng, Lukas M. Klees, Rachel Langenbacher, Lan Yao, and Ming An**

Abstract: *The pH low insertion peptide (pHLIP) offers the potential to deliver drugs selectively to the cytoplasm of cancer cells based on tumor acidosis. The WT pHLIP inserts into membranes with a pH_{50} of 6.1, while most solid tumors have extracellular pH (pH_e) of 6.5–7.0. To close this gap, a SAR study was carried out to search for pHLIP variants with improved pH response. Replacing Asp25 with α-aminoadipic acid (Aad) adjusts the pH_{50} to 6.74, matching average tumor acidity, and replacing Asp14 with γ-carboxyglutamic acid (Gla) increases the sharpness of pH response (transition over 0.5 instead of 1 pH unit). These effects are additive: the Asp14Gla/Asp25Aad double variant shows a pH_{50} of 6.79, with sharper transition than Asp25Aad. Furthermore, the advantage of the double variant over WT pHLIP in terms of cargo delivery was demonstrated in turn-on fluorescence assays and anti-proliferation studies (using paclitaxel as cargo) in A549 lung cancer cells at pH 6.6.*

One approach to targeted cancer therapy relies on the use of a drug carrier that can distinguish between normal and cancer cells. The recent success of antibody–drug conjugates validates this approach.[1] However, targeting specific tumor-associated proteins can be hampered by heterogeneity among cells within a tumor[2] and rapid development of resistance.[3] An alternative approach is to target cancer cells based on universal features of the tumor microenvironment (for example, hypoxia),[4] which may have broad applications in many different types of cancers. Tumor acidosis is such a property that may be exploited.[5] Many solid tumors have interstitial acidity (pH_e of 6.5–7.0), compared to normal tissue pH_e of 7.2–7.5, whereas the intracellular pH of cancer and healthy cells are similar (both pH 7.0–7.5).[5,6]

Tumor acidosis results from a) the altered metabolism of cancer cells, that is, ATP production via glycolysis with reduced rate of respiration, at first, in response to hypoxia (the Pasteur effect), but eventually even under conditions of plentiful oxygen (the Warburg effect); and b) a fast rate of metabolism coupled with poor clearance of waste products.[7] Low tumor pH_e may confer growth advantages on cancer cells, as healthy tissue and their extracellular matrix remodel under acidic stress, clearing space for local tumor invasion and eventual metastasis.[8] Cancer cells living in acidic and hypoxic environments are especially resistant to radiation and chemotherapy, which in turn contribute to tumor recurrence.[4,7a,9] Thus using pHLIP to target acidic cancer cells for destruction can offer a complementary approach to established therapies.

At the physiological pH of 7.2–7.5, pHLIP is unstructured in solution (State I in Figure 1) or peripherally bound to membrane surfaces (State II); under slightly acidic conditions, pHLIP inserts across a lipid bilayer, forming a transmembrane (TM) helix (State III).[10] The insertion is unidirectional with C-terminus translocated across the membrane,[10c,11] rapid (equilibrium reached in minutes),[12] and mediated mainly by the protonations of Asp14 and Asp25 carboxyl sidechains in the TM region.[10b,13] Both D- and L-pHLIP peptides can target acidic tumors in vivo.[13,14] Furthermore, pHLIP does not cause membrane leakage,[11a,15] and no toxic effects have been oberved in cell culture (up to 10 μM) or mice (5 mg kg^{-1}).[11a,13,16] Owing to its small size (36–38 amino acids, ≈4 KD), pHLIP can penetrate to the core of tumor where hypoxia and acidosis are most prominent.[16]

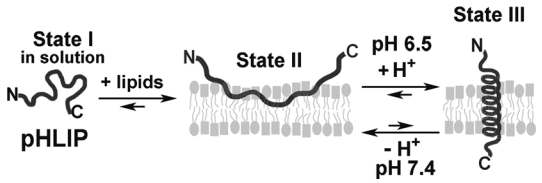

Figure 1. Insertion of the pHLIP peptide into a membrane in response to acidity.

[*] Dr. J. O. Onyango,[+] M. S. Chung,[+] C.-H. Eng, L. M. Klees, R. Langenbacher, Prof. Dr. M. An
Department of Chemistry
State University of New York (SUNY), Binghamton University
P.O. Box 6000, Binghamton, NY 13902 (USA)
E-mail: aming@binghamton.edu
Prof. Dr. L. Yao
Department of Physics, Applied Physics and Astronomy
State University of New York (SUNY), Binghamton University
P.O. Box 6000, Binghamton, NY 13902 (USA)
E-mail: lanyao@binghamton.edu
[+] These authors contributed equally to this work.

[**] We thank Prof. Dr. Donald M. Engelman (Yale) for discussion and support and Prof. Dr. Eriks Rozners and Prof. Dr. Susan Bane (both of SUNY-Binghamton) for frequent use of their fluorimeter and plate reader, respectively. We also thank Raemer J. Lapid (for assistance in processing data), Rebecca A. Chandler, Meghan M. Bell, Vladyslav Nazarenko, Ilana G. Bandler (for assistance in cell assays), and Emma A. Gordon (for assistance in synthesis). This work was supported by SUNY-Binghamton University (BU) (Start-up funds to M.A. and L.Y., various financial supports to J.O.O., L.M.K., and M.S.C., HHMI-BU undergraduate summer fellowships to C-H.E. and R.L.), NIH (R01-GM073857 for training of M.A. and initial work), and NSF grant CHE-0922815 for the Regional NMR Facility (600 MHz instrument) at SUNY-Binghamton.

Supporting information for this article is available on the WWW under http://dx.doi.org/10.1002/anie.201409770.

These properties favor pHLIP as a drug carrier worthy of further development.

One challenge in targeting tumor acidosis is the small pH difference between healthy tissue and tumor. Thus, the drug carrier should be a pH sensor with sharp transition. Previous efforts in targeting tumor pH_e have been focused on pH-responsive polymers. Taking advantage of the facts that the imidazole side-chain of histidine is protonated to the imidazonium cation with a pK_a of 7.0 (neutral to positive at low pH_e) whereas certain sulfonamides have pK_a of 6.8 for the NH α-proton (negative to neutral at low pH_e), Bae and co-workers engineered a wide variety of polymer-based molecular devices (for example, micelles) and behaviors (such as unveiling of cell-penetrating peptides) to respond to the slightly acidic environment of tumors for drug delivery.[17] Another recently reported approach is based on the acid-catalyzed, β-carboxyl neighboring-group assisted hydrolysis of *N*-alkyl maleamic acids (negative to positive conversion in response to low pH_e).[18] However, the stability of this charge reversal system at pH 7.4 is a concern.[18a,b,e] Compared to these polymer-based systems, pHLIP is simpler and more chemically defined, which can have significant practical advantages in drug carrier development.

When cargo, such as a small dye molecule, a cyclic peptide, or a peptide nucleic acid (PNA), is attached to the C-terminus of pHLIP, it can be carried across the membrane during pHLIP insertion.[11,20] Thus, pHLIP not only can target cancer cells based on low tumor pH_e but also deliver the cargo directly into the cytoplasm. Such insertion-mediated delivery of phalloidin (and other toxins) inhibited the proliferation of cancer cells in a pH-dependent fashion.[20a–c] Furthermore, when many copies of pHLIP are attached to the surface of 13 nm gold[21] or 140 nm mesoporous silica nanoparticles,[22] they seem to be able to work in concert to bring such large cargo into cells. Recently, as the first example of in vivo efficacy, pHLIP-mediated delivery of PNA (anti-miR) silenced miR-155 onco-miR in a mouse lymphoma model.[23]

We believe pHLIP also presents an opportunity to improve cancer chemotherapy. Many drugs, such as paclitaxel (Taxol) or doxorubicin, have dose-limiting toxicity in off-target sites (for example, bone marrow, heart). Our goal is to use pHLIP to deliver such drugs selectively to cancer cells. In the current study we aim to create pHLIP variants that insert more effectively in response to tumor pH_e through incorporation of noncanonical amino acids. The best of these variants are further evaluated in cellular assays to demonstrate its advantage over WT pHLIP.

The pHLIP peptide is derived from the TM helix C of bacteriorhodopsin and has the following sequence: GGEQN-PIYWARYA**D**WLFTTPLLLL**D**LALLVDADEGT.[10b] For the original "WT" pHLIP, the apparent pH_{50} of insertion (that is, the pH at which 50% of pHLIP are in the inserted State III) across 1-palmitoyl-2-oleoylphosphatidylcholine (POPC) membrane is about 6.1 (Figure 3).[10b,19,24] When pHLIP peptides interact with cells, insertion may take place at plasmamembrane or endosomal membranes, and likely both.[25] Given its pH_{50} even the WT pHLIP is able to efficiently deliver cargo into the cytoplasm in response to endosomal acidity. Yet drug delivery by insertion in the plasma-membrane in response to tumor pH_e can benefit from increased pH_{50} because most solid tumors exhibit an average pH_e of 6.8.[5,6]

Our structure–activity relationship (SAR) study contains 9 novel pHLIP variants, the structures of which are shown in Figure 2. Their insertion behavior into POPC membrane were

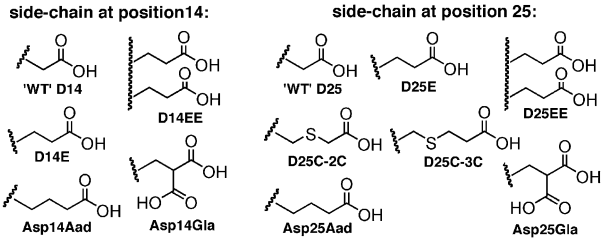

Figure 2. Side-chain structural variations at pHLIP position 14 and 25. WT, D14E, and D25E are previously known.[10b,19]

characterized using established Trp fluorescence methods.[19–20,24,26] The basis of the assay is that pHLIP insertion (State II to III in Figure 1) leads to an increase in Trp fluorescence intensity and a blue-shift in emission λ_{max}, reflecting the more hydrophobic environment the Trp side-chains experience after insertion (especially W15). Further, circular dichroism (CD) measurements were carried out to confirm the pH-dependent conformational change: random coil in States I and II but α-helical in State III.[10b,19] The apparent pH_{50} values are calculated by fitting the transition curve of "pH vs. λ_{max}" (Figure 3 left column) to the Henderson–Hasselbalch equation (albeit with pH_{50} in place of pK_a):

$$\lambda_{max} = \lambda_{max\text{-III}} + (\lambda_{max\text{-II}} - \lambda_{max\text{-III}})/(1 + 10^{n(pH_{50} - pH)}) \quad (1)$$

where n is the Hill coefficient (which reflects the sharpness or cooperativity of insertion into POPC membrane), and $\lambda_{max\text{-II}}$ and $\lambda_{max\text{-III}}$ are the wavelengths of maximum emission in the membrane-bound State II and the inserted State III, respectively. For each novel variant, the Trp fluorescence assay is repeated at least three times and the average pH_{50} and Hill coefficient values are reported along with standard deviations (s.d.) in Table 1.

The D25E and D14E variants have been described to insert with pH_{50} of about 6.4–6.5.[19] To minimize aggregation, we carried out experiments with lower ionic strength (11 mM vs. 68 mM) and peptide concentration (2 μM vs. 7 μM) than reported procedures. Under such conditions, D25E and D14E showed pH_{50} of 6.27 ± 0.03 and 6.14 ± 0.05, respectively (Table 1; see the Supporting Information, Table S1 for sequence details and Figure S2 for Trp fluorescence and CD data). The D25E variant is an important precedent for our SAR study as it demonstrates that lengthening the D25 side-chain can increase pH_{50}.

To find out to what extent can side-chain extension at position 25 be tolerated, the Cys side-chain of a D25C pHLIP was lengthened by reaction with bromoacetic acid or 3-bromopropionic acid to give variant D25C-2C or D25C-3C (Figure 2). The D25C-2C has a pH_{50} of 6.05 ± 0.04 and a Hill

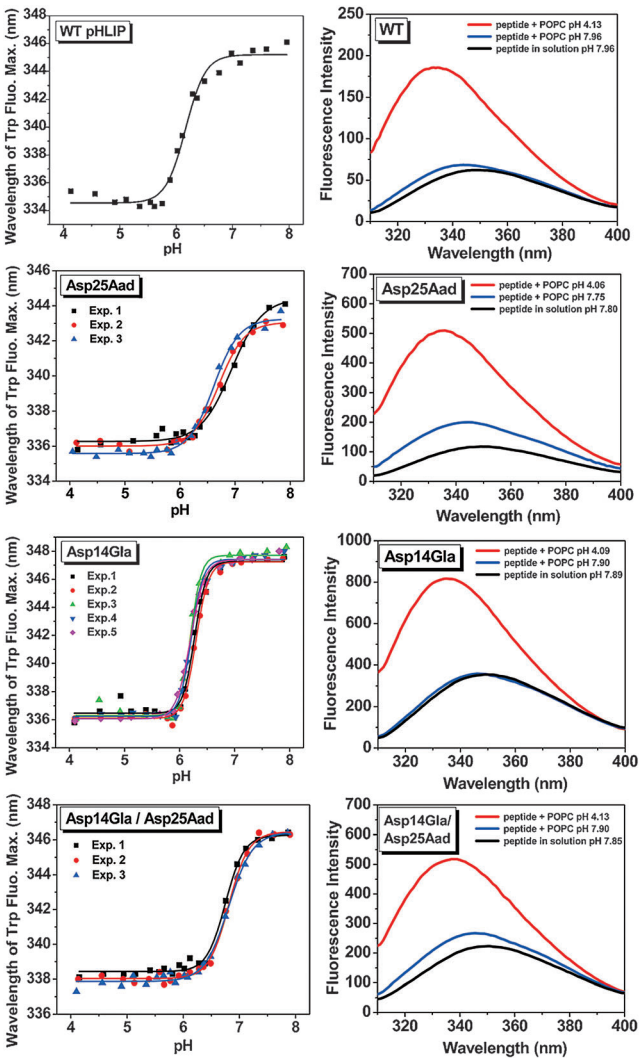

Figure 3. Trp fluorescence of Asp25Aad, Asp14Gla, and Asp14Gla/Asp25Aad pHLIP variants, which show improved pH response at the tumor pH_e range of 6.5–7.0. Left column (top to bottom): insertion is monitored through Trp fluorescence λ_{max} blue-shift (different colors denote experimental repeats); compared to the WT, the Asp25Aad insertion shifted to a higher pH range closely matching tumor acidity but suffers from poor cooperativity; the Asp14Gla variant has strikingly sharp pH response; the Asp14Gla/Asp25Aad double variant maintains a high pH_{50} of 6.8 with coopravity restored to WT level. Right column: For the pHLIP variants studied, Trp fluorescence spectra of State I (black), II (blue), and III (red) show an increase in fluorescence intensity and λ_{max} blue-shift from State II to State III (that is, pHLIP insertion into POPC liposome membrane).

coefficient of 2.44 ± 0.10 (similar to WT), with pH-dependent helix formation characteristic of a pHLIP (as confirmed by CD; Supporting Information, Figure S2). However, the D25C-3C variant lost the coil-to-helix transition: its CD signal is already weakly helical at pH 8 and there is no increase in helicity at pH 4 (Supporting Information, Figure S2). Compared to State I, its "State II" Trp fluorescence shows significant increase in intensity and emission λ_{max} blue-shift (Supporting Information, Figure S2). Further λ_{max} blue-shift from "State II" to "III" is unusually narrow (5.5 nm for D25C-3C vs. 8–12 nm for all other variants), and the pH vs. λ_{max} transition is poorly defined ($n = 0.9$). Such data indicate that D25C-3C is not a typical pHLIP, possibly because the additional methylene group increases the tendency of aggregation. In D25C-2C, the electron withdrawing ability of the sulfur atom increases side-chain acidity, shifting the pH_{50} unfavorably down. However, D25C-2C gave hope that its carbon isostere Asp25Aad would still behave as a pHLIP.

Indeed, Asp25Aad pHLIP has clear coil-to-helix transition from State II to III (Supporting Information, Figure S1). More importantly, Asp25Aad has a pH_{50} of 6.74 ± 0.14 (Figure 3), closely matching average tumor pH_e in vivo. Asp25Aad is also consistent with the trend observed from WT to D25E: as the number of methylene groups in the side-chain increased, the pH_{50} rose (WT 6.16 to D25E 6.27 to Asp25Aad 6.74). Since the peptide backbone is electron-withdrawing, as it became more distant, the innate acidity of the side-chain carboxylic acid decreased, shifting pH_{50} up. When D14 instead of D25 is replaced with Aad, the resulting Asp14Aad variant has proper pH-dependent insertion (Supporting Information, Figure S3), yet the pH_{50} is only 6.37 ± 0.03. Therefore, factors other than the inherent side-chain pK_a, such as the precise location and the polarity of the protonation environment in State II, also influence the pH_{50}. The side-chain at position 25 seems to dominate the setting of pH_{50}.

However, the Hill coefficient of Asp25Aad insertion into POPC membrane is 1.73 ± 0.17, lower than that of WT (2.48). Insertion at neutral pH may hamper the selectivity of pHLIP-mediated drug delivery. Thus, a sharp pH-response, that is, insertion over a narrow pH range, is desirable. Engelman and co-workers postulated that more carboxylic acid residues in the TM region may increase the insertion cooperativity.[19] Although their attempts at introducing additional carboxyl group were not successful, we thought to revisit this hypothesis. First, the Asp14 or Asp25 residue was replaced with a pair of Glu residues, giving the variants D14EE or D25EE. CD confirmed that D14EE and D25EE have pH-dependent coil-to-helix transition characteristic of a pHLIP (Supporting Information, Figure S3). But to our disappointment, D14EE has a pH_{50} of 6.19 ± 0.04 with a Hill coefficient of 1.41 ± 0.02 while D25EE has a pH_{50} of 6.60 ± 0.14 with a Hill coefficient of 1.34 ± 0.26. Both of these variants insert over a wider range than WT pHLIP (Supporting Information, Figure S3).

Next, the D14 or D25 residue was substituted with the noncanonical amino acid Gla, which has two carboxyl groups appended to the γ-carbon of the side-chain (Figure 2), resulting in the variants Asp14Gla or Asp25Gla. Compared with D14EE and D25EE variants, this modification allows for more precise introduction of the additional carboxyl group at locations critical for pHLIP insertion. CD showed that Asp14Gla and Asp25Gla both have clearly defined pH-dependent coil-to-helix transition (Supporting Information, Figures S1 and S3). Asp25Gla turned out to be unremarkable, with pH_{50} of 6.20 ± 0.02 and a Hill coefficient of 1.90 ± 0.19 (Supporting Information, Figure S3). On the other hand, Asp14Gla has a pH_{50} of 6.24 ± 0.05 but with a transition Hill coefficient of 3.98 ± 0.40 (Figure 3). Thus, the Asp14Gla variant has the sharpest pH response recorded to date for

Table 1: Insertion pH_{50}, Hill coefficient *n*, and Trp fluorescence $\lambda_{max\text{-}II/III}$ of pHLIP variants studied.

pHLIP variants	pH_{50}	*n*	$\lambda_{max\text{-}II}$ [nm]	$\lambda_{max\text{-}III}$ [nm]
WT	6.16	2.48	345.2	334.5
D25E	6.27 ± 0.03	2.14 ± 0.20	344.9 ± 0.3	334.9 ± 0.2
D14E	6.14 ± 0.05	2.47 ± 0.33	345.6 ± 0.3	335.6 ± 0.2
D25C-2C	6.05 ± 0.04	2.44 ± 0.10	344.6 ± 1.2	334.5 ± 0.5
D25C-3C	6.18	0.9	343.5	338.0
Asp25Aad	6.74 ± 0.14	1.73 ± 0.17	344.5 ± 1.9	336.1 ± 0.4
Asp14Aad	6.37 ± 0.03	2.05 ± 0.13	344.4 ± 1.5	336.0 ± 0.6
Asp25Gla	6.20 ± 0.02	1.90 ± 0.19	346.6 ± 0.6	335.1 ± 0.2
Asp14Gla	6.24 ± 0.05	3.98 ± 0.40	347.4 ± 0.2	336.2 ± 0.2
D25EE	6.60 ± 0.14	1.34 ± 0.26	345.0 ± 1.5	335.5 ± 1.6
D14EE	6.19 ± 0.04	1.41 ± 0.02	346.7 ± 1.0	335.6 ± 0.3
Asp14Gla/Asp25Aad	6.79 ± 0.04	2.38 ± 0.30	346.4 ± 0.1	338.1 ± 0.3

a pHLIP, with insertion occurring over half pH unit vs. one pH unit for the WT.

To see whether higher insertion pH_{50} and sharper pH response could be tuned separately in an additive fashion, the Asp14Gla/Asp25Aad double variant was tested. The CD data showed clear pH-dependent coil-to-helix transition characteristic of a pHLIP (Supporting Information, Figure S1); and indeed, this double variant maintains a high insertion pH_{50} of 6.79 ± 0.04, similar to that of Asp25Aad, while the transition Hill coefficient is restored to 2.38 ± 0.30, close to the WT level of sharpness in pH-response (Figure 3).

With this best variant in hand, we set out to demonstrate its advantage over WT pHLIP in cultures of A549 human lung cancer cells. WT or Asp14Gla/Asp25Aad pHLIP containing C-terminal Lys and Cys residues were used to synthesize turn-on fluorescence probes (with rhodamine TAMRA attached to the Lys side-chain by an amide bond and quencher QSY9 attached to the adjacent Cys side-chain through a disulfide bond) and pHLIP-paclitaxel conjugates (the drug paclitaxel is conjugated to the Cys side-chain through a disulfide bond traceless linker; Figure 4). Details of their syntheses are described in the Supporting Information, Schemes S1 and S2.

In the self-quenched turn-on fluorescence probe, the quencher QSY9 serves as a model cargo of intracellular drug delivery. As the disulfide linker is selectively cleaved inside of cells, presumably by glutathione (GSH), QSY9 release would lead to dequenching and increase in TAMRA fluorescence (Figure 4a), thus reporting the level of pHLIP insertion in cellular membranes (because the C-terminus is translocated across membrane during pHLIP insertion). In the WT vs. Asp14Gla/Asp25Aad comparison, data shown in Figure 4a establish that dequenching levels (and thus inferred pHLIP insertion levels) are considerably higher for the double variant at all acidic pHs but similar at neutral pH. In particular, the pH 7.4 vs. 6.6 comparison reveals that the amount of pH-dependent cargo release, which represents the therapeutic window in pHLIP-mediated drug delivery in vivo, is much greater for the double variant (9.2- vs. 5.2-fold) than the WT (5.9- vs. 4.3-fold). Thus, the Asp14Gla/Asp25Aad variant should be able to deliver drug in a more pH-dependent fashion than WT.

To test this hypothesis in antiproliferation assays, the drug paclitaxel is conjugated to pHLIP by an ester–disulfide linkage on its C2′ OH (Figure 4b; Supporting Information, Scheme S2). As attachment at this site would interfere with paclitaxel binding to tubulin,[27] a traceless linker is constructed following known methods[28] in which upon cleavage of the disulfide bond in cells, the resulting linker SH group would cyclize onto the paclitaxel C2′ ester carbonyl to release the cargo exactly as paclitaxel (Figure 4b). This trace-less linker strategy was tested in a chemical cleavage assay by incubating WT

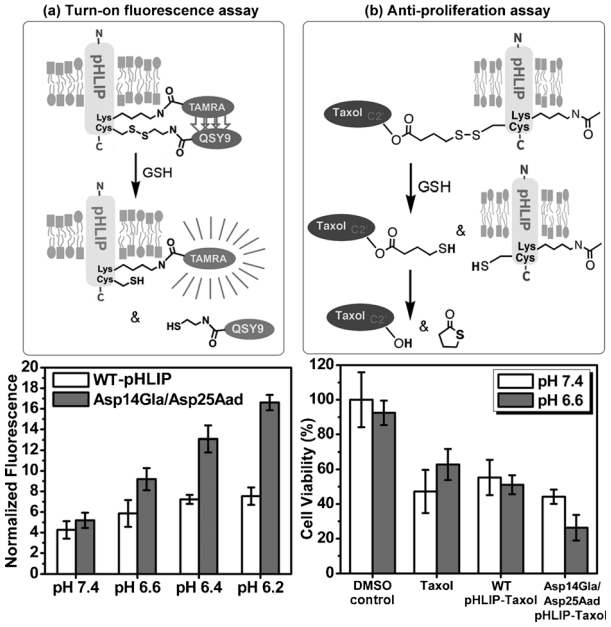

Figure 4. Evaluation of WT pHLIP vs. Asp14Gla/Asp25Aad variant in A549 cancer cells. a) Turn-on fluorescence assays: At all acidic pHs, Asp14Gla/Asp25Aad pHLIP released more disulfide-linked QSY9 quencher than WT pHLIP. The TAMRA fluorescence levels plotted were measured 72 h after treatment with 0.5 μM of self-quenched probe for 30 min ($n = 8$, error bar is s.d.). b) Anti-proliferation assays: At pH 6.6, Asp14Gla/Asp25Aad pHLIP-paclitaxel inhibited the growth of A549 cancer cells to a greater extent than either WT pHLIP-paclitaxel or the free drug itself (30 min treatment with 0.5 μM of drug or pHLIP-drug, $n = 8$, error bar is s.d.).

pHLIP-paclitaxel (4 μM) with glutathione (11 mM) in DPBS buffer (pH 7.6). Cargo release was monitored with HPLC, which showed that within 2 h up to 90% of paclitaxel cargos were released as the free drug (Supporting Information, Figure S4). In the growth inhibition assay, A549 cells were treated with WT or Asp14Gla/Asp25Aad pHLIP-paclitaxel (0.5 μM, 30 min) at the simulated tumor pH of 6.6–6.7 (pH measured before and after experiment) or the healthy tissue pH of 7.4. The results of these experiments are shown in Figure 4b. At pH 6.6, the double variant has decisive advantage over WT pHLIP in delivering paclitaxel into the cell, both in terms of absolute amount delivered (thus leading to more growth inhibition) and pH dependence. Interestingly,

even WT pHLIP-paclitaxel can inhibit cell growth as well as free drug but the pH-dependence is largely absent. On the other hand, Asp14Gla/Asp25Aad pHLIP-paclitaxel can inhibit cell growth to a greater extent than free drug (74% vs. 37% growth inhibition) at pH 6.6 and its anti-proliferative effects are very pH sensitive: 74% inhibition at pH 6.6 vs. 56% at pH 7.4.

In summary, to find pHLIP variants with improved insertion properties for drug delivery at tumor average pH_e of 6.8, we carried out a SAR study in which the D14 and D25 residues critical for insertion were modified. The variants D25EE, Asp25Aad, and Asp14Gla/Asp25Aad insert with pH_{50} of 6.60, 6.74, and 6.79, respectively. These three variants insert into POPC membrane at higher pH than all previously known pHLIP peptides. Thus, they may insert more effectively at the tumor pH_e range of 6.5–7.0, with the potential to deliver more drugs into the cytoplasm of cancer cells via plasmamembrane insertion. To reduce pHLIP-mediated drug delivery at neutral pH (which may lead to off-target effects in healthy tissues), insertion over a narrow pH range is desirable. To this end, we found that the Asp14Gla variant can insert into membrane with the sharpest pH-response observed so far for a pHLIP peptide: over half a pH unit vs. one pH unit for WT. This Asp14Gla variant may improve pHLIP-based tumor imaging by reducing background signals. Thus, adding carboxyl group to the 14th position side-chain can sharpen the pH response while lengthening the side-chain at position 25 can raise the pH_{50} of insertion. The Asp14Gla/Asp25Aad double variant shows that these effects are independent of each other and can be used additively to tune for desired pHLIP insertion properties. Furthermore, the successful introduction of additional carboxyl groups in the TM region, as in D25EE and Asp14Gla, may also improve pHLIP solubility and reduce aggregation, which are parameters critical for future applications. We have also shown that the double variant Asp14Gla/Asp25Aad has considerble advantage over WT pHLIP in cargo delivery at true tumor pH_e of 6.6, as demonstrated with turn-on fluorescence assays and anti-proliferation studies in A549 cells using paclitaxel as a model drug.

Experimental Section

Details of the sequences of pHLIP variants (and their characterization by mass spectrometry), synthetic derivatizations that led to D25C-2C and D25C-3C variants, capping of C-terminal Lys and Cys side-chains of D14E and D25E variants, syntheses of WT and Asp14Gla/Asp25Aad pHLIP turn-on fluorescence probes and pHLIP-paclitaxel conjugates, paclitaxel cargo release test, Trp fluorescence experiments, CD measurements, liposome preparation, cell culture (materials, instruments and cell line), turn-on fluorescence, and anti-proliferation assays with A549 cells, can be found in the Supporting Information.

Received: October 5, 2014
Revised: November 27, 2014
Published online: January 29, 2015

Keywords: biosensors · cancer · drug delivery · peptides · pH low insertion peptide

[1] a) P. D. Senter, E. L. Sievers, *Nat. Biotechnol.* **2012**, *30*, 631 – 637; b) E. L. Sievers, P. D. Senter, *Annu. Rev. Med.* **2013**, *64*, 15 – 29.
[2] Y. H. Bae, *J. Controlled Release* **2009**, *133*, 2 – 3.
[3] M. E. Gorre, M. Mohammed, K. Ellwood, N. Hsu, R. Paquette, P. N. Rao, C. L. Sawyers, *Science* **2001**, *293*, 876 – 880.
[4] W. R. Wilson, M. P. Hay, *Nat. Rev. Cancer* **2011**, *11*, 393 – 410.
[5] a) L. E. Gerweck, K. Seetharaman, *Cancer Res.* **1996**, *56*, 1194 – 1198; b) J. L. Wike-Hooley, J. Haveman, H. S. Reinhold, *Radiother. Oncol.* **1984**, *2*, 343 – 366.
[6] a) X. Zhang, Y. Lin, R. J. Gillies, *J. Nucl. Med.* **2010**, *51*, 1167 – 1170; b) Z. M. Bhujwalla, D. Artemov, P. Ballesteros, S. Cerdan, R. J. Gillies, M. Solaiyappan, *NMR Biomed.* **2002**, *15*, 114 – 119.
[7] a) R. A. Gatenby, R. J. Gillies, *Nat. Rev. Cancer* **2004**, *4*, 891 – 899; b) I. F. Tannock, D. Rotin, *Cancer Res.* **1989**, *49*, 4373 – 4384.
[8] a) V. Estrella, T. Chen, M. Lloyd, J. Wojtkowiak, H. H. Cornnell, A. Ibrahim-Hashim, K. Bailey, Y. Balagurunathan, J. M. Rothberg, B. F. Sloane, J. Johnson, R. A. Gatenby, R. J. Gillies, *Cancer Res.* **2013**, *73*, 1524 – 1535; b) I. F. Robey, B. K. Baggett, N. D. Kirkpatrick, D. J. Roe, J. Dosescu, B. F. Sloane, A. I. Hashim, D. L. Morse, N. Raghunand, R. A. Gatenby, R. J. Gillies, *Cancer Res.* **2009**, *69*, 2260 – 2268.
[9] G. Helmlinger, F. Yuan, M. Dellian, R. K. Jain, *Nat. Med.* **1997**, *3*, 177 – 182.
[10] a) Y. K. Reshetnyak, O. A. Andreev, M. Segala, V. S. Markin, D. M. Engelman, *Proc. Natl. Acad. Sci. USA* **2008**, *105*, 15340 – 15345; b) J. F. Hunt, P. Rath, K. J. Rothschild, D. M. Engelman, *Biochemistry* **1997**, *36*, 15177 – 15192; c) Y. K. Reshetnyak, M. Segala, O. A. Andreev, D. M. Engelman, *Biophys. J.* **2007**, *93*, 2363 – 2372.
[11] a) Y. K. Reshetnyak, O. A. Andreev, U. Lehnert, D. M. Engelman, *Proc. Natl. Acad. Sci. USA* **2006**, *103*, 6460 – 6465; b) D. Thévenin, M. An, D. M. Engelman, *Chem. Biol.* **2009**, *16*, 754 – 762.
[12] O. A. Andreev, A. G. Karabadzhak, D. Weerakkody, G. O. Andreev, D. M. Engelman, Y. K. Reshetnyak, *Proc. Natl. Acad. Sci. USA* **2010**, *107*, 4081 – 4086.
[13] O. A. Andreev, A. D. Dupuy, M. Segala, S. Sandugu, D. A. Serra, C. O. Chichester, D. M. Engelman, Y. K. Reshetnyak, *Proc. Natl. Acad. Sci. USA* **2007**, *104*, 7893 – 7898.
[14] R. C. Adochite, A. Moshnikova, S. D. Carlin, R. A. Guerrieri, O. A. Andreev, J. S. Lewis, Y. K. Reshetnyak, *Mol. Pharm.* **2014**, *11*, 2896 – 2905.
[15] M. Zoonens, Y. K. Reshetnyak, D. M. Engelman, *Biophys. J.* **2008**, *95*, 225 – 235.
[16] Y. K. Reshetnyak, L. Yao, S. Zheng, S. Kuznetsov, D. M. Engelman, O. A. Andreev, *Mol. Imaging Biol.* **2011**, *13*, 1146 – 1156.
[17] a) E. S. Lee, Z. Gao, Y. H. Bae, *J. Controlled Release* **2008**, *132*, 164 – 170; b) J. Hu, S. Miura, K. Na, Y. H. Bae, *J. Controlled Release* **2013**, *172*, 69 – 76; c) E. S. Lee, Z. Gao, D. Kim, K. Park, I. C. Kwon, Y. H. Bae, *J. Controlled Release* **2008**, *129*, 228 – 236.
[18] a) J. Z. Du, X. J. Du, C. Q. Mao, J. Wang, *J. Am. Chem. Soc.* **2011**, *133*, 17560 – 17563; b) J. Z. Du, T. M. Sun, W. J. Song, J. Wu, J. Wang, *Angew. Chem. Int. Ed.* **2010**, *49*, 3621 – 3626; *Angew. Chem.* **2010**, *122*, 3703 – 3708; c) Z. X. Zhou, Y. Q. Shen, J. B. Tang, M. H. Fan, E. A. Van Kirk, W. J. Murdoch, M. Radosz, *Adv. Funct. Mater.* **2009**, *19*, 3580 – 3589; d) Y. Lee, K. Miyata, M. Oba, T. Ishii, S. Fukushima, M. Han, H. Koyama, N. Nishiyama, K. Kataoka, *Angew. Chem. Int. Ed.* **2008**, *47*, 5163 – 5166; *Angew. Chem.* **2008**, *120*, 5241 – 5244; e) Y. Lee, S. Fukushima, Y. Bae, S. Hiki, T. Ishii, K. Kataoka, *J. Am. Chem. Soc.* **2007**, *129*, 5362 – 5363.
[19] M. Musial-Siwek, A. Karabadzhak, O. A. Andreev, Y. K. Reshetnyak, D. M. Engelman, *Biochim. Biophys. Acta Biomembr.* **2010**, *1798*, 1041 – 1046.

[20] a) M. An, D. Wijesinghe, O. A. Andreev, Y. K. Reshetnyak, D. M. Engelman, *Proc. Natl. Acad. Sci. USA* **2010**, *107*, 20246 – 20250; b) D. Wijesinghe, D. M. Engelman, O. A. Andreev, Y. K. Reshetnyak, *Biochemistry* **2011**, *50*, 10215 – 10222; c) A. Moshnikova, V. Moshnikova, O. A. Andreev, Y. K. Reshetnyak, *Biochemistry* **2013**, *52*, 1171 – 1178; d) A. G. Karabadzhak, M. An, L. Yao, R. Langenbacher, A. Moshnikova, R. C. Adochite, O. A. Andreev, Y. K. Reshetnyak, D. M. Engelman, *ACS Chem. Biol.* **2014**, *9*, 2545 – 2553.

[21] A. Davies, D. J. Lewis, S. P. Watson, S. G. Thomas, Z. Pikramenou, *Proc. Natl. Acad. Sci. USA* **2012**, *109*, 1862 – 1867.

[22] Z. Zhao, H. Meng, N. Wang, M. J. Donovan, T. Fu, M. You, Z. Chen, X. Zhang, W. Tan, *Angew. Chem. Int. Ed.* **2013**, *52*, 7487 – 7491; *Angew. Chem.* **2013**, *125*, 7635 – 7639.

[23] C. J. Cheng, R. Bahal, I. A. Babar, Z. Pincus, F. Barrera, C. Liu, A. Svoronos, D. T. Braddock, P. M. Glazer, D. M. Engelman, W. M. Saltzman, F. J. Slack, *Nature* **2014**, DOI: 10.1038/nature13905, published online 17 November 2014.

[24] J. Fendos, F. N. Barrera, D. M. Engelman, *Biochemistry* **2013**, *52*, 4595 – 4604.

[25] L. Yao, J. Daniels, D. Wijesinghe, O. A. Andreev, Y. K. Reshetnyak, *J. Controlled Release* **2013**, *167*, 228 – 237.

[26] a) F. N. Barrera, J. Fendos, D. M. Engelman, *Proc. Natl. Acad. Sci. USA* **2012**, *109*, 14422 – 14427; b) G. A. Caputo, E. London, *Biochemistry* **2004**, *43*, 8794 – 8806.

[27] D. G. Kingston, *J. Nat. Prod.* **2000**, *63*, 726 – 734.

[28] E. A. Dubikovskaya, S. H. Thorne, T. H. Pillow, C. H. Contag, P. A. Wender, *Proc. Natl. Acad. Sci. USA* **2008**, *105*, 12128 – 12133.

